Generation of sub-wavelength and super-resolution longitudinally polarized non-diffraction beam using lens axicon

K. B. Rajesh and P. M. Anbarasan

Department of Physics, Periyar University, Salem 636011, India

Received April 21, 2008

It is well known that a light spot of sub-wavelength will diverge in all directions. In this letter, A method is presented for generating sub-wavelength (0.44λ) longitudinally polarized beam, which propagates without divergence over lengths of about 2λ in free space. This is achieved by a high numerical aperture (NA) lens axicon that utilizes spherical aberration to duplicate the performance of an axicon and to create an extended focal line.

OCIS codes: 320.7120, 260.1440.
doi: 10.3788/COL20080610.0785.

Most of the near field applications such as optical data storage, biomedical imaging, and lithography demands sub-wavelength beam with large depth of focus. Overcoming the limits imposed by diffraction has been the aim of many research during the last decades. The super resolution was extensively investigated using amplitude apertures[1,2], phase apertures[2], or their combination[3,4]. It was observed that a strong longitudinal component appears at the focal region of a tightly focused laser beam[5−7]. It also arises with focusing of radially polarized light[8−10]. The longitudinal field can be suppressed or enhanced by amplitude, polarization, and phase modulations of the incident beam. For example, a longitudinal field can be completely suppressed in an azimuthally polarized beam[10,11]. Several methods to enhance the longitudinal field component have been suggested[12,13], however all of them have insufficient optical efficiency (on the level of a few percents) and non-uniform axial field strength. An axicon is an optical element generating a narrow focal line along the optical axis. The axicon, energy wise, is the most efficient method for generating a diffraction free beam. The focal line generated by the axicon can be approximated by a zero-order Bessel-type beam that preserves its transverse distribution along the axis. The idea of using spherical aberration to produce an axicon from ordinary lenses was first suggested by Steel in 1960[14]. It has been thoroughly investigated both analytically and numerically[15−17]. However, this analysis only specifies the focal length and the amount of spherical aberration required. The experimental aspect of designing the lens axicon was investigated in Ref. [18]. The advantage of such a system is that spherical surfaces can be routinely produced in any optical workshop, so the lens axicon is easy and inexpensive to manufacture. A possible design, presented in this letter, is a cemented doublet-lens axicon, where the virtual focal segment created by the aberrated diverging lens can be converted to a real focal segment, of the forward type with a nano-scale resolution, by adding a high numerical aperture (NA) converging lens. In addition, we consider only the systems that comprise a third-order spherical aberration diverging lens and a perfect high-NA converging lens illuminated by a radially polarized beam. The schematic diagram of the lens axicon is shown in Fig. 1. It is shown that for radially polarized incidenting, a Fresnel zone plate (FZP) is superior to a high NA lens in focusing properties[19]. This is due to a large apodization factor of FZP for high NA, which gives larger weight to higher spatial components. Owing to the phase nature of FZP, the resolution is improved without reduction in intensity. However, compared with FZP, the proposed lens axicon system is simple to fabricate, mount, and align. The analysis was performed on Richards and Wolf's vectorial diffraction method[20] which was widely used for high-NA focusing systems at arbitrary polarized incidenting[21,22]. In the case of the radially polarized incidenting, adopting the cylindrical coordinates r, z and the notations used in Ref. [23], radial and longitudinal components of the electric field $E_r(r,z)$ and $E_z(r,z)$ in the vicinity of the focal spot can be written as

$$E_r(r,z) = A\int_{\alpha_1}^{\alpha_2} \cos^{1/2}(\theta)\sin(2\theta)\times l(\theta) \times J_1(kr\sin\theta)\mathrm{e}^{ikz\cos\theta}\mathrm{d}\theta,$$

$$E_z(r,z) = 2iA\int_{\alpha_1}^{\alpha_2} \cos^{1/2}(\theta)\sin^2(\theta)\times l(\theta) \times J_0(kr\sin\theta)\mathrm{e}^{ikz\cos\theta}\mathrm{d}\theta, \quad (1)$$

where α_1 distinguishes the presence or absence of annulus, $\alpha_2 = \arcsin(\mathrm{NA}/n)$, and n is the index of refraction between the lens and the sample. $J_0(x)$ and $J_1(x)$ denote Bessel functions of the zero and first order. Function $l(\theta)$ describes amplitude modulation. For illumination by a Bessel-Gaussian beam with its waist in the pupil this function is given by

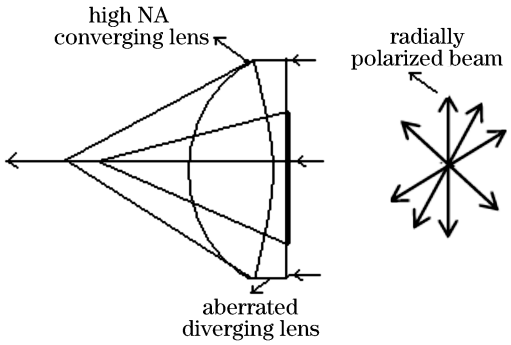

Fig. 1. Schematic diagram of a lens axicon.

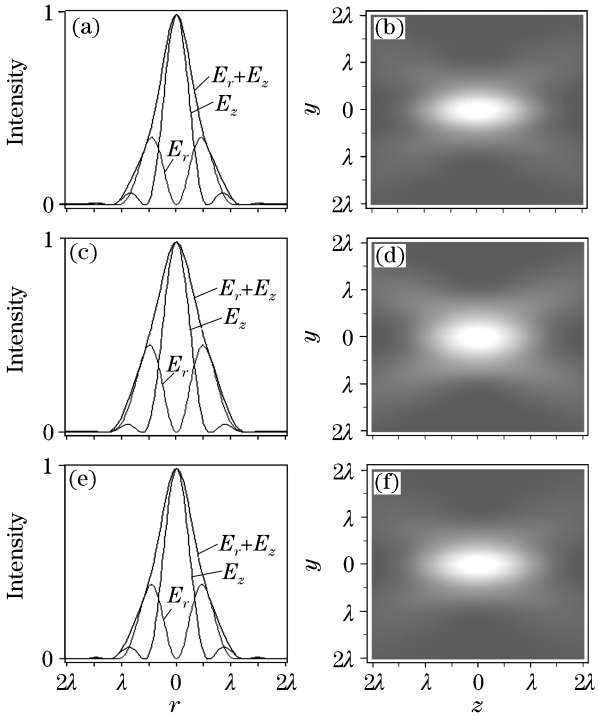

Fig. 2. Intensity profiles of the radial component, longitudinal component, and the total field on the focal plane of the NA = 0.90 lens for radial polarized (a) plane, (c) Gaussian, and (e) Bessel-Gaussian beam. (b), (d), and (f) are their corresponding contour plots of total intensity.

$$l(\theta) = \exp\left[\left[-\xi_1^2\left(\frac{\sin\theta}{\sin\alpha}\right)^2\right] J_1\left(2\xi_2\frac{\sin\theta}{\sin\alpha}\right)\right], \qquad (2)$$

for a Gaussian beam with its waist in the pupil

$$l(\theta) = \exp\left[-\left(\frac{\xi_3\sin\theta}{\sin\alpha_2}\right)^2\right], \qquad (3)$$

and for the plane beam $l(\theta) = 1$. ξ_1, ξ_2, ξ_3 are the parameters that denote the ratio of the pupil diameter to the beam diameter, and in our calculation, we take them as unity. We perform the integration numerically by using parameters $\lambda = 405$ nm, NA = 0.90 ($\alpha_2 = 64.15$), and $n = 1$. The corresponding field distribution is shown in Fig. 2. From Figs. 2(a), (c), and (e), it is observed that the intensities of longitudinal components are high for all three types of beam illumination, but the parasite radial field intensities are about 36.3%, 43.6%, and 39.2% corresponding to plane, Gaussian, and Bessel-Gaussian beam. This radial field leads to a broadening of the total intensity distribution. As a result, the total intensity spot sizes become 0.83λ, 0.98λ, and 0.88λ corresponding to plane, Gaussian, and Bessel-Gaussian illumination. It is observed that the full-width at half-maximum (FWHM) is the smallest in the case of uniform amplitude profile, while the Gaussian beam results in the largest FWHM. Moreover, the contour plots of the total intensity distribution in yz plane in Figs. 2(b), (d), and (f) show that the field changes from a converging spherical wavefront to a diverging wavefront within a very short distance ($\sim \lambda$). Thus to have a good longitudinally polarized beam with better depth of focus, one should suppress the radial field component. We show that it is possible in lens axicon to make a doublet of aberrated diverging lens and a high-NA converging lens. The intensity distribution of the lens axicon is evaluated by replacing the function $l(\theta)$ by the function $l(\theta)T(\theta)$, where $T(\theta)$ is the non paraxial transmittance function of the thin aberrated diverging lens

$$T(\theta) = \exp\left(Ik\left(\beta\left(\frac{\sin(\theta)}{\sin\alpha_2}\right)\right)^4 + \left(\frac{1}{2f}\left(\frac{\sin(\theta)}{\sin\alpha_2}\right)^2\right)\right), \qquad (4)$$

where $k = 2\pi/\lambda$, f is the focal length, and β is the aberration coefficient. In our calculation, we take $f = 18.4$ mm, $\beta = 6.667 \times 10^{-5}$ mm^{-3}, and $n = 1.5$. This results in an equiconcave diverging lens which is simple to

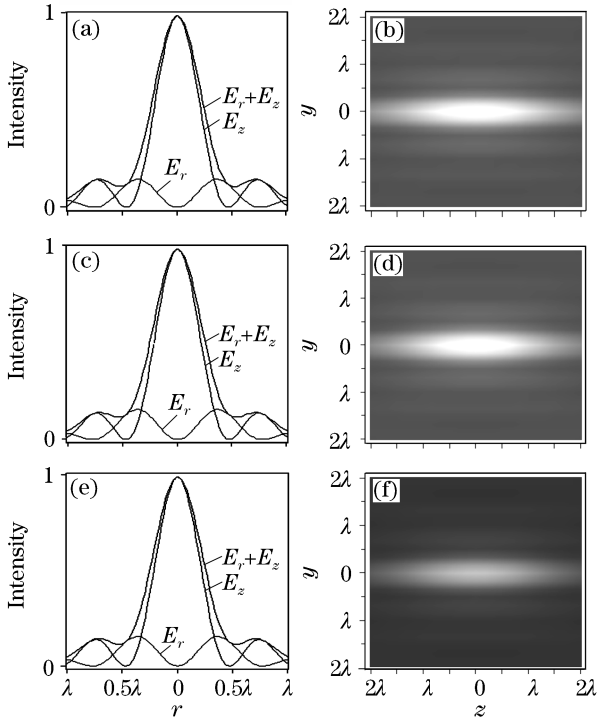

Fig. 3. Intensity profiles of the radial component, longitudinal component, and the total field on the focal plane of the lens axicon for radial polarized (a) plane, (c) Gaussian, and (e) Bessel-Gaussian beam. (b), (d), and (f) are their corresponding contour plots of total intensity.

manufacture[15]. The focal distribution of the lens axicon is calculated by including the transmission function of the aberrated diverging lens on the aperture of the high-NA focusing lens. The intensity profiles of the radial component, the longitudinal component, and the total field of the longitudinally polarized beam in the focal cross section are shown in Fig. 3. It is observed that the parasite radial field intensities are reduced to 15.3%, 16%, and 15.6% and the spot sizes are 0.43λ, 0.44λ, and 0.43λ, corresponding to plane, Gaussian and Bessel-Gaussian beam, respectively. The intensity contour plots shown in Figs. 3(b), (d), and (f) depict that the spot sizes are constant within certain region, implying that the diffractive spreading is eliminated and a non-diffractive beam propagates in this region. The non-diffractive region extends to 2λ, 2λ, and 1.8λ corresponding to plane, Gaussian, and Bessel-Gaussian beam. Outside the region where the axial intensity is constant, the field diverges almost as fast as it does in the original system.

In conclusion, a method to obtain a sub-wavelength and super-resolution longitudinally polarized non-diffracting beam within a limited space is proposed and demonstrated numerically. This is achieved by placing a diverging aberrated lens in front of a high-NA converging lens. The method of our calculation is based on vector diffraction theory, which is suitable to be used in both paraxial and non-paraxial focusing and imaging system. We expect such a beam with small spot size and long depth of focus can be widely used in application such as data storage, biomedical imaging, laser drilling, and machining.

The authors are grateful to the reviewers for their helpful comments. This work was supported by the University Research Fellowship offered by Periyar University. K. B. Rajesh's e-mail address is rajeskb@gmail.com.

References

1. C. J. R. Sheppard and A. Choudhury, Appl. Opt. **43,** 4322 (2004).
2. L. E. Helseth, Opt. Commun. **191,** 161 (2001).
3. C. Liu and S.-H. Park, Opt. Lett. **29,** 1742 (2004).
4. Y. Xu, J. Singh, C. J. R. Sheppard, and N. Chen, Opt. Express **15,** 6409 (2007).
5. C. J. R. Sheppard, Microwaves, Optics and Acoustics **2,** 163 (1978).
6. D. Ganic, X. Gan, and M. Gu, Opt. Express **11,** 2747 (2003).
7. K. G. Lee and H. W. Kihm, Nature Photon. **1,** 53 (2006).
8. Z. Bouchal and M. Olivik, J. Mod. Opt. **42,** 1555 (1995).
9. C. J. R. Sheppard and P. Török, Optik **104,** 175(1997).
10. C. J. R. Sheppard and S. Saghafi, Opt. Lett. **24,** 1543 (1999).
11. G. Machavariani and Y. Lumer, Opt. Lett. **32,** 1468 (2007).
12. C. J. R. Sheppard, J. Opt. Soc. Am. A **18,** 1579 (2001).
13. R. Dorn, S. Quabis, and G. Leuchs, J. Mod. Opt. **50,** 1917 (2003).
14. W. H. Steel, "Colloquia of the international commission for optics: optics in metrology" P. Mollet ed. (Pergamon, Oxford, UK, 1960) pp.181 − 192.
15. Z. Jaroszewicz and J. Morales, J. Opt. Soc. Am. A **15,** 2383 (1998).
16. Z. Jaroszewicz and J. Morales, J. Opt. Soc. Am. A **16,** 191 (1999).
17. J. Pu, H. Zhang, and S. Nemoto, Opt. Eng. **39,** 803 (2000).
18. A. Burvall, K. Kołcz, Z. Jaroszewicz, and A. T. Friberg, Appl. Opt. **43,** 4838 (2004).
19. N. Davidson and N. Bokor, Opt. Lett. **29,** 1318 (2004).
20. B. Richards and E. Wolf, Proc. R. Soc. London **A253,** 358 (1959).
21. C.-C. Sun and C.-K. Liu, Opt. Lett. **28,** 99 (2003).
22. T. G. Jabbour and S. M. Kuebler, Opt. Express **14,** 1033 (2006).
23. K. S. Youngwotrh and T. G. Brown, Opt. Express **7,** 77 (2000).